

On A Comparison of Numerical Solution Methods for General Transport Equation on Cylindrical Coordinates

Ali ATEŞ^{1,*}, Omer ALTUN² and Adem KILICMAN²

¹ Mechanical Engineering Department, Technology Faculty, Seluk University, Konya, Turkey.

² Mathematics Department and Institute for Mathematical Research, University Putra Malaysia, 43400 UPM, Serdang, Selangor, Malaysia

Received: 12 Dec. 2016, Revised: 15 Jan. 2017, Accepted: 30 Jan. 2017

Published online: 1 Mar. 2017

Abstract: In this study, the general transport equation was subjected to discretization by using the central difference, upwind, hybrid, power-law, exponential scheme and QUICK scheme methods and then solved by using a program prepared in Delphi programming software. In the solution, three different grid systems of 80x100, 160x200 and 320x400 from nodal points were used. The numerical results obtained for Peclet number values of -2, 0, 2, 10 and 20 we presented graphically. The obtained results indicate that hybrid and power-law yield better results as compared to the other discretization methods. The GCI analysis was also provided that 160 x 200 grid system is suitable for such a solution.

Keywords: General transport equation, Discretization, GCI analysis.

1 Introduction

Convection deals with molecular and mass flow movement of a matter. Mass flow transfer refers to movement of materials within two mixed fluids or in a single fluid due to differences in concentration in different areas of the fluid. There is similarity between Fourier heat transfer law and diffusion. Just as temperature difference is an effective factor that constrains heat transfer, so is concentration difference because the latter hinders mass flow rate in a fluid.

There is a physical similarity between heat transfer by convection and mass transfer. In nature wherever there is convection in a medium diffusion (i.e. dispersion of matter) will also be spoken of. That's why in most of the problems regarding fluid flow, convection and diffusion are investigated together.

In literature, the general transport equation is seen to have been used in various engineering fields. In a study by Aslam and De [1] the convection-diffusion equation was solved by using different solution methods of finite elements method and the results of the different methods were compared. Wang and Wen-Qia [2] generated an alternative solution from the Crank-Nicolson method with variable coefficients to solve the convection-diffusion

equation. Karaa and Zhang [3], used the fourth order scheme and iteratively solved a two dimension convection-diffusion equation with a variable coefficient. In order to reduce wrong diffusion in numerical solutions, Virag and Trincas [4] proposed a control volume method suitable for one dimensional simple difference schemes. They compared the results of their study with the results from the exact solution and exponential scheme methods.

Whereas in this study, the general transport equation which is widely used in heat transfer and mass flow problems was solved numerically by using different discretization methods and different grid numbers.

The general transport equation can be expressed as,

$$\frac{\partial(\rho\phi)}{\partial t} + \text{div}(\rho u\phi) = \text{div}(\Gamma \text{grad}\phi) + S_\phi. \quad (1)$$

Here, the terms in the equation are respectively, time dependent term, convection term, diffusion term and source term. Further ϕ is a characteristic feature of a fluid and can hence be chosen in different ways, Γ is diffusion coefficient, ρ represents fluid density while u is velocity gradient. In a two dimensional cylindrical coordinate system with a laminar, incompressible, axially symmetrical and continuous inner pipe flow having a

* Corresponding author e-mail: aates@selcuk.edu.tr

negligible source term and its diffusion coefficient considered constant, equation 1 above can be written in the following open format;

$$\rho \left[\frac{\partial}{\partial x} (u\phi) + \frac{1}{r} \frac{\partial}{\partial r} (rv\phi) \right] - \Gamma \left[\frac{\partial^2 \phi}{\partial x^2} + \frac{1}{r} \frac{\partial}{\partial r} \left(r \frac{\partial \phi}{\partial r} \right) \right] = 0. \quad (2)$$

If this equation is applied to the control volume surfaces on the two dimensional cylindrical coordinates system at a given grid system (Figure 1) and then integrated numerically, the equation 3 can be obtained.

$$\rho \{ r_p [(u\phi)_e - (u\phi)_w] \Delta r + [(rv\phi)_n - (rv\phi)_s] \Delta x \} - \Gamma \left\{ r_p \left[\left(\frac{\partial \phi}{\partial x} \right)_e - \left(\frac{\partial \phi}{\partial x} \right)_w \right] \Delta r + \left[\left(r \frac{\partial \phi}{\partial r} \right)_n - \left(r \frac{\partial \phi}{\partial r} \right)_s \right] \Delta x \right\} = 0. \quad (3)$$

The e, w, n, and s subscripts in this equation respectively, denote east, west, north and south and were used in order to make the equation more suitable to computer notation. Here, line x is axial direction and r is radial direction.

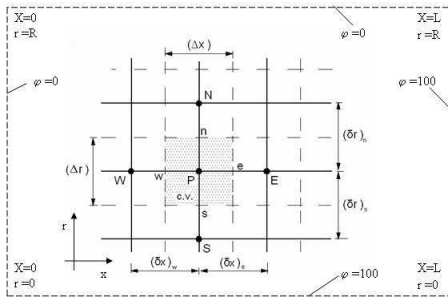


Figure 1. Control volume and boundary conditions for two dimensional cylindrical coordinate's grid system.

For the point derivative expression

$$\phi_e = (\phi_E - \phi_P) / (\delta x)_e$$

and moreover, if variable $F_e = (\rho u)_e$,

$$D_e = (\Gamma / \delta x)_e$$

$$Pe = F / D$$

is applied to all the control volume and to all the surfaces then the equation takes the following form;

$$\frac{r_p}{2} [F_e (\phi_E + \phi_P) - F_w (\phi_P + \phi_W)] \Delta r + [r_n F_n (\phi_N + \phi_P) - r_s F_s (\phi_P + \phi_S)] \Delta x - r_p [D_e (\phi_E - \phi_P) - D_w (\phi_P - \phi_W)] \Delta r - [r_n D_n (\phi_N - \phi_P) - r_s D_s (\phi_P - \phi_S)] \Delta x = 0 \quad (4)$$

and in this way, the equation suits well to the computer program index notation.

2 Central difference scheme

In this method, the arithmetic mean of the fluid is taken as a fluid feature of the interface for the control volume of the interface and centre point considered. According to this;

$$\phi_e = (\phi_P + \phi_E) / 2$$

$$\phi_w = (\phi_W + \phi_P) / 2$$

$$\phi_n = (\phi_P + \phi_N) / 2$$

$$\phi_s = (\phi_S + \phi_P) / 2.$$

If substituted into equation 4, and if the coefficients aE, aW, aN, aS are defined for the fluid features at grid points, the centre difference equation can then be written as;

$$a_P \phi_P = a_W \phi_W + a_E \phi_E + a_S \phi_S + a_N \phi_N. \quad (5)$$

In equation 5 these coefficients were defined as;

$$a_E = D_e - F_e / 2$$

$$a_W = D_w + F_w / 2$$

$$a_N = D_n - F_n / 2$$

$$a_S = D_s + F_s / 2$$

and

$$a_P = a_W + a_E + a_S + a_N + (F_e - F_w) + (F_n - F_s).$$

In the literature, it is described that Peclet number in ranges out of $2 < Pe < 2$ do not present accurate results for the centre difference scheme [5].

3 Upwind Difference Scheme

In this method, depending on flow direction, the fluid characteristic takes features of the adjacent upper flow zone neighbour of the control volume. In other words, the fluid takes properties of the control volume one step

before its own control volume. With this, if $F_e > 0$, $F_w > 0$, $F_n > 0$ and $F_s > 0$, then $\phi_e = \phi_P$, $\phi_w = \phi_W$, $\phi_n = \phi_P$ and $\phi_s = \phi_S$. Again if $F_e < 0$, $F_w < 0$, $F_n < 0$ and if $F_s < 0$, then $\phi_e = \phi_E$, $\phi_w = \phi_P$, $\phi_n = \phi_N$ and $\phi_s = \phi_P$. According to this, for $F_e > 0$, $F_w > 0$, $F_n > 0$, $F_s > 0$ in equation 5, the coefficients take these forms

$a_E = D_e$, $a_W = D_w + F_w$, $a_N = D_n$, $a_S = D_s + F_s$ and for $F_e < 0$, $F_w < 0$, $F_n < 0$, $F_s < 0$, they become $a_E = D_e - F_e$, $a_W = D_w$, $a_N = D_n - F_n$, $a_S = D_s$. In order to write these coefficients in more compact forms, the following notation can be preferred;

$$a_e = D_e + \max[0, -F_e], \quad a_w = D_w + \max[F_w, 0], \quad a_n = D_n + \max[0, -F_n], \quad a_s = D_s + \max[F_s, 0]$$

In this way, the condition of ‘same signs in coefficients’, which is one of the four basic conditions of the upwind scheme, will be covered.

4 Hybrid Difference Scheme

Essentially, this method has emerged as a combination of the centre difference and upwind schemes. Depending on the condition of the Pe number, the system can sometimes operate as a centre difference scheme and sometimes as an upwind scheme. Provided that the basic equation remains the same, the coefficients change as follows:

$$a_e = \max\left[-F_e, \left(D_e - \frac{F_e}{2}\right), 0\right], \quad a_w = \max\left[F_w, \left(D_w + \frac{F_w}{2}\right), 0\right],$$

$$a_n = \max\left[-F_n, \left(D_n - \frac{F_n}{2}\right), 0\right], \quad a_s = \max\left[F_s, \left(D_s + \frac{F_s}{2}\right), 0\right].$$

5 Power-law Difference Scheme

This is a method that resembles the hybrid difference scheme but gives more accurate results. In this method, results that are relatively close to those obtained with the exact method can be achieved. The coefficients are as follows:

$$a_e = \max[-F_e, 0] + D_e \cdot \max\left[0, (1 - 0.1|Pe_e|)^2\right], \quad a_w = \max[F_w, 0] + D_w \cdot \max\left[0, (1 - 0.1|Pe_w|)^2\right],$$

$$a_n = \max[-F_n, 0] + D_n \cdot \max\left[0, (1 - 0.1|Pe_n|)^2\right], \quad a_s = \max[F_s, 0] + D_s \cdot \max\left[0, (1 - 0.1|Pe_s|)^2\right].$$

6 Exponential Scheme

The exponential scheme is developed from the solution of an exact solution of a differential equation. Actually; this method is given to show how close the Power-law Difference Scheme is to the exact solution. As seen in the graphs of the results of this study, shortly, the difference between power-law and exponential scheme is so small that can be neglected. The equation coefficients for this method are given in exponential form.

$$a_e = \frac{F_e}{\exp\left(\frac{F_e}{D_e}\right) - 1}, \quad a_w = \frac{F_w \cdot \exp\left(\frac{F_w}{D_w}\right)}{\exp\left(\frac{F_w}{D_w}\right) - 1}, \quad a_n = \frac{F_n}{\exp\left(\frac{F_n}{D_n}\right) - 1}, \quad a_s = \frac{F_s \cdot \exp\left(\frac{F_s}{D_s}\right)}{\exp\left(\frac{F_s}{D_s}\right) - 1}$$

7 QUICK Scheme

The QUICK (the quadratic upstream interpolation for convective kinetics) scheme, basically, exhibits some

distinctions as compared to the other methods. In this method, two adjacent control volumes of the flow zone are taken into account in the calculations. In this way, a total of 6 adjacent control volumes (3 horizontal and 3 vertical) become involved in the discretization process. It is for this reason that changes are observed not only in the coefficients but also in the main equation itself. Like this; If

$$a_P \phi_P = a_W \phi_W + a_E \phi_E + a_S \phi_S + a_N \phi_N + a_{WW} \phi_{WW} + a_{SS} \phi_{SS} \quad (6)$$

The coefficients satisfy the following relations;

$$a_E = D_e - \frac{3}{8} F_e, \quad a_W = D_w + \frac{6}{8} F_w + \frac{1}{8} F_e,$$

$$a_{WW} = -\frac{1}{8} F_w, \quad a_N = D_n - \frac{3}{8} F_n,$$

$$a_S = D_s + \frac{6}{8} F_s + \frac{1}{8} F_n, \quad a_{SS} = -\frac{1}{8} F_s \quad \text{and}$$

$$a_P = a_W + a_E + a_S + a_N + a_{WW} + a_{SS} + (F_e - F_w) + (F_n - F_s).$$

If; $F_e < 0$, $F_w < 0$, $F_n < 0$, $F_s < 0$ then

$$a_P \phi_P = a_W \phi_W + a_E \phi_E + a_S \phi_S + a_N \phi_N + a_{EE} \phi_{EE} + a_{NN} \phi_{NN} \quad (7)$$

Coefficients;

$$a_E = D_e - \frac{6}{8} F_e - \frac{1}{8} F_w, \quad a_W = D_w + \frac{3}{8} F_w, \quad a_{EE} = \frac{1}{8} F_e$$

$$a_N = D_n - \frac{6}{8} F_n - \frac{1}{8} F_s, \quad a_S = D_s + \frac{3}{8} F_s, \quad a_{NN} = \frac{1}{8} F_n$$

and

$$a_P = a_W + a_E + a_S + a_N + a_{EE} + a_{NN} + (F_e - F_w) + (F_n - F_s).$$

Any result beyond Peclet number range of $-8/3 < Pe < 8/3$ for the QUICK scheme is not accurate [6]. Standard QUICK scheme was developed by Hayese *et al.*, [7].

8 Computational Method

By using a computer program prepared by using Delphi software, solutions for grid network system formed of 80x100 (coarse grid), 160x200 (medium grid) and 320x400 (fine grid) nodal points were generated by using the above described discretization methods. Gauss-Siedal iteration method was used for solution of the equations. To achieve more accurate graphic printouts, Lagrange interpolation method was used to concentrate the values in between the main points. The results obtained directly in graphic forms were compared with each other.

Computations were made by using values corresponding to Peclet numbers -2, 0, 2, 10, 20 and some of the results were given. Results for any selected Peclet number can be obtained.

In this study, $u=2$ m/s and $v=0.8$ m/s were used. ϕ was assumed to vary between 0 and 100 and the r and x lines were set at 1 unit and 10 unit distances respectively. Assumptions were made such that, for $x=0$ $\phi=0$, for $r=0$, $\phi=100$, for $x=L$ $\phi=100$, and for $r=R$ $\phi=0$. The values given are not specific values and can be selected as required for a given physical problem.

9 Results and Discussion

Numerical solutions are verified by means of a transient post processing tool based on the generalized Richardson extrapolation and the Grid Convergence Index (GCI) [8]. Sample solutions were made by using coarse and fine grids assuming the selected grid system as medium. A second order method is used in GCI analysis by taking the grid refinement ratio as 2.0 [8] and therefore the grid sizes are doubled in coarse and halved in fine grid systems in both axial and radial coordinates. The quantities of interest for comparison are general solution values at half of axial size. Root mean square values of general solution values in terms of grid size are given Table 1. The parameter values used in the sample calculations and the results of GCI analysis are given in Table 2. The relatively low values of relative errors, ε , and of GCI between medium and fine grids suggest that the 160x200 grid resolution is quite acceptable. The computations may be assumed within the asymptotic range and no further grid refinement is necessary.

Table 1. Root mean square values of general solution values.

Grid	Grid size ($r \times x$)	ϕ_{rms}
Coarse	80 x 100	68.6104
Medium	160 x 200	72.4061
Fine	320 x 400	74.3972

Table 2. The relative errors and Grid Converge Index measures for all grid schemes.

Grid	ε	GCI
Coarse-Medium	-0.052422	0.173519
Medium-Fine	-0.026763	0.088586

In Figure 2, variation of x - axis and r -axis for the obtained ϕ values is shown from each discretization method for $Pe=2$. Variation of ϕ starts from a far distant point along the x -axis. This condition can be explained that the effects of convection are slow at the beginning. The variation in the radial direction is relatively

proportional. Just as it can be seen from the graphs, the results obtained from each method are close to each other. However; the results from the upwind scheme method are somehow different. It is normal for the curves to take a horizontal trend in low Peclet number values. Beside this, the event does not necessarily make the upwind scheme to yield more accurate results as compared to the other methods.

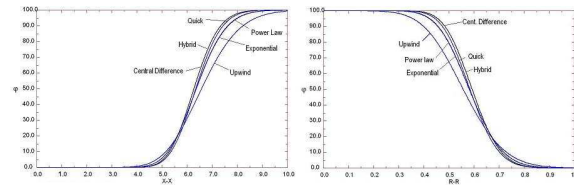


Figure 2. Variation of average values of ϕ along x - and r - axes for each discretization method ($Pe=2$).

In Figure 3, the overall results obtained for three different grid systems along x -axis are shown. The number of nodes in the coarse grid system was 80x100, for the medium grid system, the number was 160x200, while for fine grid system 320x400 was used. These values were obtained through trial and error method.

In Figure 4. The overall results obtained for three different grid systems along r -axis are shown. It is clearly seen in both figures that as the number of nodes increases exact solution is approached more closely. In addition, the curves for upwind scheme in both figures are clearly seen to differ from the other methods. Together with this, attention is drawn from similarities of the results from the central difference method and those from the hybrid solution. Similar trend is observed between the power-law and exponential scheme methods.

According to figure 5, the effects of various Pe number values on the axial direction were investigated separately for each method. The study was made on values corresponding to Pe numbers -2, 0, 2, 10 and 20 and the results obtained were presented on the graphs. The Central difference method does not give correct results for Pe values less than -2 and greater than +2. It is for this reason that only values for Pecletin -2, 0 and +2 are seen on the Central difference scheme. Similarly, the Quick discretization method does not yield results for Pecletin values smaller than -8/3 and larger than, +8/3; and this is why there are no higher Pe values on the graph

of Quick scheme. Given that $Pe = \frac{F}{D}$ and $F = \rho u$ negative Pe values show that the flow moves towards the opposite direction. For this reason, the curves obtained at $Pe=-2$ are located at the far right of the graphs because the flow moves from right to left. $Pe=0$ means the flow is stagnant. In other words, the effect of convection is zero. This makes the variation in ϕ to follow parabolic path.

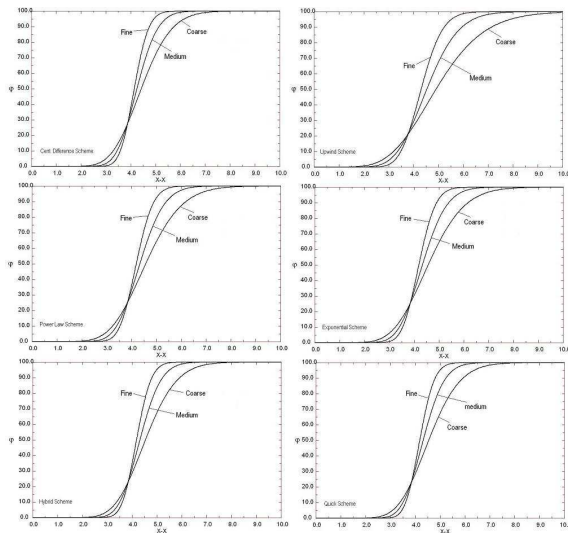


Figure 3. Variation of ϕ for every discretization method along x-axis ($Pe=2$).

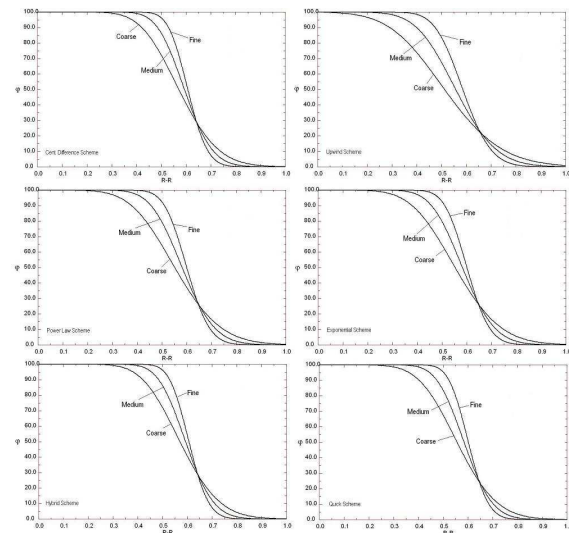


Figure 4. Variation of ϕ for every discretization method along r-axis ($Pe=2$).

That is, no turning point is observed here as seen in the other curves. It is also clear that larger Pecletin values cause extensive convection effects. It can thus be said that progress was previously achieved for large Pe values. However; this effect is not obvious for Peclet values greater than 10. And this can be seen clearly on the graphs. The curves for Power-law, Exponential and Hybrid scheme solutions overlap each other at $Pe=10$ and $Pe=20$.

In figure 6, effects of various Pe values on radial direction for every method are shown. Here the most remarkable aspect is the fact that, for positive Pe numbers, the ϕ does not undergo any significant changes from the pipe axis up to areas close to the pipe wall and that near the wall, the ϕ value drops abruptly. And this gives a hint that there are profound convection effects nearby the pipe wall due to strong Pe number on the inner parts.

The parabolic curve obtained at $Pe=0$ exhibits a horizontal trend on areas near the pipe axis. The ϕ value drops sharply at the rate of about 15% along the areas very near to the pipe axis. Due to the fact that no convection effects are observed at $Pe=0$, then these changes can be said to have been imposed by diffusion. It can be said that diffusion effects are weak on the areas where the curve undergoes a horizontal trend.

10 Conclusions

By evaluating this study as a whole, it is clear that the most ideal method among the differential equations discretization methods is the power-law difference scheme. In this method, different coefficients between Pe

values of -10 and $+10$ are used, and by using various coefficients out of these values for Pe values between $-\infty$ and $+\infty$, results very close to the exact solution can be obtained. Hybrid discretization operates like the central difference method between $-2 \leq Pe \leq 2$ and out of this ranges, it works like the upwind discretization method (Patankar, 1980). Because it is a discretization method formed by combining two methods after covering their respective weaknesses, it becomes a strong discretization method. In order to obtain more accurate results from these two methods, it is important that the method with the larger absolute Pe value be used.

Number of nodes in the grid system affects the solution results. In this study, the lowest nodal number was considered as 80×100 . Solution accuracies obtained with nodal points lower than this value are not reliable. On average, the study was conducted with nodal number of 160×200 . This number is sufficient for reliable results. However; more accurate results were obtained from a grid system formed from 320×400 nodal points. However, with this point, it takes much time to accomplish that solution.

In addition, a study similar to this can also be conducted for cylindrical coordinates where the source term is considered. Moreover; another study can be made with a three dimensional Cartesian coordinates system.

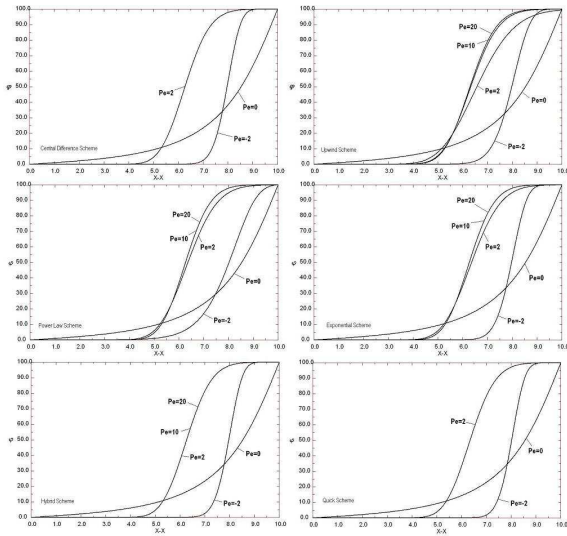


Figure 5. Comparison of variations of ϕ for every discretization method along x-direction drawn for Pe values of Pe=-2, Pe=0, Pe=2, Pe=10 and Pe=20.

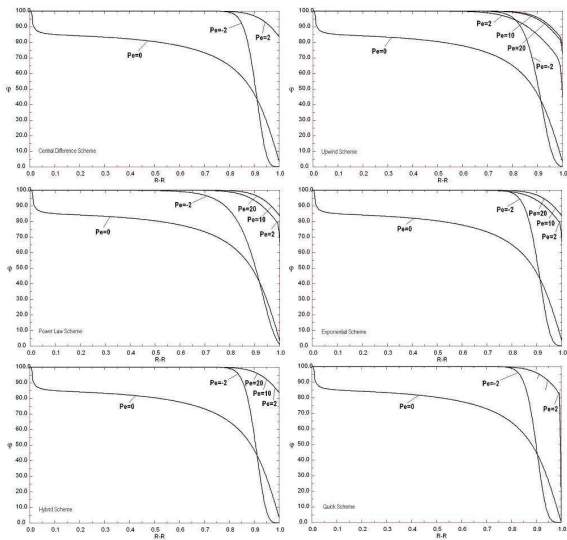


Figure 6. Comparison of variations of ϕ for every discretization method along r-direction drawn for Pe values of Pe=-2, Pe=0, Pe=2, Pe=10 and Pe=20.

NOMENCLATURE

a Coefficients of discretization equation

D Coefficient $D = \Gamma / \delta x$ or $D = \Gamma / \delta r$

E,e East

F Coefficient $F = \rho * u$ or $F = \rho * v$

Fs Safety factor

GCI Grid Convergence Index

- h Grid spacing ($h = \Delta x$)
- L Total axial length (m)
- N,n North
- p Spatial order of accuracy
- Pe Peclet number, $Pe = F/D$
- R Radius (m)
- r Radial direction
- r Grid refinement factor
- S Source term
- S,s South
- u Velocity gradient
- u Axial velocity component ($m.s^{-1}$)
- v Radial velocity component ($m.s^{-1}$)
- W,w West
- x Axial direction
- Δr Radial step size (m)
- δr Radial position difference (m)
- Δx Axial step size (m)
- δx Axial position difference (m)
- ε Relative error
- ϕ General solution variable
- Γ Diffusion coefficient
- ρ Density ($kg.m^{-3}$)
- Subscripts**
- 3, 2, 1 Subscripts of coarse, medium and fine (or mesh level course to fine)
- rms Root mean square

References

- [1] Aslam, A., De, S., (2005) A comparison of several numerical methods for the solution of the convection-diffusion equation using the method of finite spheres, *Comput. Mech.* V. 36: pp. 398-407.
- [2] Weng, Wen-Qia, (2003) Alternating segment Crank-Nicolson method for solving convection-diffusion equation with variable coefficient, *Applied Mathematics and Mechanics*, v 24, n 1, pp. 32-42.
- [3] Karaa, S., Zhang, J., (2002) Methods for Solving Variable Coefficient Convection-Diffusion Equation with a Fourth-Order Compact Difference Scheme, *An International Journal Computers & Mathematics with Application*, V. 44, pp. 457-479.
- [4] Virag, Z., Trincas, G., (1994) An improvement of the exponential differencing scheme for solving the convection-diffusion equation, *Advances in Engineering Software*, V. 19, Issue 1, pp. 1-20.
- [5] Patankar, S. V., (1980) *Numerical heat transfer and fluid flow*, Hemisphere publishing corporation, Chap. 5, pp. 79-111.
- [6] Versteeg, H. K., Malalasekera, W., (1995) *An Introduction to computational fluid dynamics The finite volume method*, Longman Group Ltd, pp. 103-134.
- [7] Hayese, T., Humphrey, J. A. C., Greif, R., (1992) A consistently formulated QUICK scheme for fast and stable convergence using finite-volume iterative calculation procedures, *J. Comput. Phys.*, V. 98, pp. 108-118.
- [8] P.J. Roache, (1994) A method for uniform reporting of grid refinement studies, *J. Fluids Eng.* 116 405-413.



Ali ATEŞ is an Assistant Professor at Selcuk University, Konya, Turkey. He received his M.Sc. degree and Ph.D from Graduate School of Natural Sciences, Selcuk University, Turkey. His research areas includes; Computational Fluid Dynamics (CFD), Numerical

Heat Transfer, Numerical Analysis for Engineering.



Omer ALTUN received M.Sc in Mathematics, (2012) and PhD in applied mathematics, (2016), University Putra Malaysia, Faculty of Science, Department of Mathematics, Malaysia. His research interests are in the areas of applied mathematics

including the differential transformation method, ordinary differential equation, boundary value problem and convolutions.



Adem KILICMAN is a full Professor at the Department of Mathematics, Faculty of Science, University Putra Malaysia. He received his B.Sc. and M.Sc. degrees from Department of Mathematics, Hacettepe University, Turkey and Ph.D from Leicester

University, United Kingdom. He has joined University Putra Malaysia in 1997 since then working with Faculty of Science and He is also an active member of Institute for Mathematical Research, University Putra Malaysia. His research area includes Functional Analysis and Topology.